Langmuir Article

pubs.acs.org/Langmuir

Wettability and Surface Free Energy of Graphene Films

Shiren Wang,*,† Yue Zhang,† Noureddine Abidi,‡ and Luis Cabrales‡

†Department of Industrial Engineering and ‡Fiber and Biopolymer Institute, Texas Tech University, Lubbock, Texas 79409

Received April 20, 2009. Revised Manuscript Received June 24, 2009

Graphene sheets were produced through chemical exfoliation of natural graphite flake and hydrazine conversion. Subsequently, graphene sheets were assembled into a thin film, and microscale liquid droplets were placed onto the film surface for measurement of wettability and contact angle. It is found that a graphene oxide sheet is hydrophilic and a graphene sheet is hydrophobic. Isolated graphene layers seem more difficult to wet in comparison to graphite, and low adhesion work was found in the graphene−liquid interface. Approximation of solid−liquid interfacial energy with the equation of state theory was applied to determine the graphene surface energy. The results indicate that surface energy of graphene and graphene oxide is 46.7 and 62.1 mJ/m^2, respectively, while natural graphite flake shows a surface free energy of 54.8 mJ/m^2 at room temperature. These results will provide valuable guidance for the design and manufacturing of graphene-based biomaterials, medical instruments, structural composites, electronics, and renewable energy devices.

Introduction

Graphene is a monolayer of carbon atoms, arranged in a honeycomb network or an unrolled single-walled carbon nanotube.[1−3] Recently, graphene has attracted a great deal of attention. Researchers at Columbia University have recently measured the mechanical properties of single graphene by nanoindentation, indicating that Young's modulus is ∼1 TPa, with a strength of 130 GPa.[4] Others measured the thermal conductivity of a graphene layer, indicating its thermal conductivity to be in the range of ∼3080−5150 W m^{-1} K^{-1}.[5−8] This extremely high thermal conductivity is comparable to current carbon nanotubes.[9] Some computational results suggested that in-plane expansion, bond-stretching, and bond-bending effects in the graphene sheet cancel out each other, leading to a negative thermal expansion coefficient in the plane graphene sheets.[10,11] Because of its planar structure, thermal contraction in graphene sheets is more obvious than in other carbon structures, such as graphite, carbon nanotubes, and diamond.[13,14] Because of its exceptional properties, graphene promises many potential applications.[15−18] Graphene has been used in organic solar cells,[19−22] field-effect transistor,[22−28] hydrogen storage,[29,30] and ultra-capacitors,[31,32] demonstrating very promising results.

The surface of a material is the most important part determining the compatibility with its environment. In many cases, although the bulk properties are excellent for a specific application, the surface may require to be modified and engineered in the desired direction. This is especially important for materials used in hybrid materials, coating, and biological media, because the surface charge, hydophilicity, and wettability are important for thrombosis formation, cell attachment, or cell proliferation.[15] As a crucial part to bridge the exceptional properties to numerous applications, the surface plays a vital role in the graphene materials. The properties of the surface, such as chemical structure, homogeneity, crystallinity, and the level of cohesive

*To whom correspondence should be addressed. E-mail: shiren.wang@ttu.edu.

(1) Geim, A. K.; Novoselov, K. S. *Nat. Mater.* **2007**, *6*, 183–191.
(2) Li, D.; Kaner, R. B. *Science* **2008**, *320*, 1170–1171.
(3) Novoselov, K. S.; Jiang, D.; Schedin, F.; Booth, T. J.; Khotkevich, V. V.; Morozov, S. V.; Geim, A. K. *Proc. Natl. Acad. Sci. U.S.A.* **2005**, *102*, 10451–10453.
(4) Lee, C.; Wei, X.; Kysar, J. W.; Hone, J. *Science* **2008**, *321*, 385–388.
(5) Ghosh, S.; Calizo, I.; Teweldebrhan, D.; Pokatilov, E. P.; Nika, D. L.; Balandin, A. A.; Bao, W.; Miao, F.; Lau, C. N. *Appl. Phys. Lett.* **2008**, *92*, 151911.
(6) Berber, S.; Kwon, Y. K.; Tomanek, D. *Phys. Rev. Lett.* **2000**, *84*, 4613–4616.
(7) Pop, E.; Mann, D.; Wang, Q.; Goodson, K.; Dai, H. J. *Nano Lett.* **2006**, *6*, 96–100.
(8) Balandin, A. A.; Ghosh, S.; Bao, W. Z.; Calizo, I.; Teweldebrhan, D.; Miao, F.; Lau, C. N. *Nano Lett.* **2008**, *8*, 902–907.
(9) Xie, S. H.; Liu, Y. Y.; Li, J. Y. *Appl. Phys. Lett.* **2008**, *92*, 243121.
(10) Schelling, P. K.; Keblinski, P. *Phys. Rev. B: Condens. Matter Mater. Phys.* **2003**, *68*, 035425.
(11) Kahaly, M. U.; Waghmare, U. V. *Bull. Mater. Sci.* **2008**, *31*, 335–341.
(12) Fasolino, A.; Los, J. H.; Katsnelson, M. I. *Nat. Mater.* **2007**, *6*, 858–861.
(13) Mounet, N.; Marzari, N. *Phys. Rev. B: Condens. Matter Mater. Phys.* **2005**, *71*, 205214.
(14) Jiang, H.; Liu, B.; Huang, Y.; Hwang, K. C. *J. Eng. Mater. Technol.* **2004**, *126*, 265–270.
(15) Chen, H.; Muller, M. B.; Gilmore, K. J.; Wallace, G. G.; Li, D. *Adv. Mater.* **2008**, *20*, 3557–3561.
(16) Shao, Q.; Liu, G.; Teweldebrhan, D.; Balandin, A. A. *Appl. Phys. Lett.* **2008**, *92*, 202108.
(17) Stankovich, S.; Dikin, D. A.; Dommett, G. H. B.; Kohlhaas, K. M.; Zimney, E. J.; Stach, E. A.; Piner, R. D.; Nguyen, S. T.; Ruoff, R. S. *Nature* **2006**, *442*, 282–286.
(18) Eda, G.; Fanchini, G.; Chhowalla, M. *Nat. Nanotechnol.* **2008**, *3*, 270–274.
(19) Wang, X.; Zhi, L. Z.; Mullen, K. *Nano Lett.* **2008**, *8*, 323–327.
(20) Wu, J. B.; Becerril, H. A.; Bao, Z. N.; Liu, Z. F; Cheng, Y. S.; Peumans, P. *Appl. Phys. Lett.* **2008**, *92*, 263302.
(21) Liu, Q.; Liu, Z. F.; Zhang, X. Y.; Zhang, N.; Yang, L. Y.; Yin, S. G.; Chen, Y. S. *Appl. Phys. Lett.* **2008**, *92*, 223303.
(22) Hong, W. J.; Xu, Y. X.; Lu, G. W.; Li, C.; Shi, G. Q. *Electrochem. Commun.* **2008**, *10*, 1555–1558.
(23) Li, X. L.; Wang, X. R.; Zhang, L.; Lee, S. W.; Dai, H. J. *Science* **2008**, *319*, 1229–1232.
(24) Mao, L. F.; Li, X. J.; Wang, Z. O.; Wang, J. Y. *IEEE Electron Device Lett.* **2008**, *29*, 1047–1049.
(25) Yoon, Y. K.; Fiori, G. L.; Hong, S. M.; Iannaccone, G.; Guo, J. *IEEE Trans. Electron Devices* **2008**, *55*, 2314–2323.
(26) Jozsa, C.; Popinciuc, M.; Tombros, N.; Jonkman, H. T.; Van Wees, B. J. *Phys. Rev. Lett.* **2008**, *100*, 236603.
(27) Ryzhii, V.; Ryzhii, M.; Satou, A.; Otsuji, T. *J. Appl. Phys.* **2008**, *103*, 094510.
(28) Ataca, C.; Akturk, E.; Ciraci, S.; Ustunel, H. *Phys. Rev. Lett.* **2008**, *93*, 043123.
(29) Lin, Y.; Ding, F.; Yakobson, B. I. *Phys. Rev. B: Condens. Matter Mater. Phys.* **2008**, *78*, 041402.
(30) Park, N.; Hong, S.; Kim, G.; Jhi, S. H. *J. Am. Chem. Soc.* **2007**, *129*, 8999–9003.
(31) Stoller, M. D.; Park, S.; Zhu, Y.; An, J.; Ruoff, R. S. *Nano Lett.* **2008**, *8*, 3498–3502.
(32) Vivekchand, S. R. C.; Rout, C. S.; Subrahmanyam, K. S.; Govindaraj, A.; Rao, C. N. R. *J. Chem. Sci.* **2008**, *120*, 9–13.

attractions between atoms and molecules, as well as the physical shape, provide a lot of information about its reaction with the surrounding environment.[33,34] Even though much of the work has been focused on graphene exfoliation, limited research has been focused on graphene surface properties. In this study, graphene is produced by graphite exfoliation, and the wettability and surface free energy is investigated by the measurement of the contact angle.

Experimental Section

Nature flake graphite, sized at 45 μm (grade 230), was kindly provided by Asbury Carbons (Asbury, NJ). Graphite (10 g), fuming nitric acid (160 mL), and sodium chloride oxide (85 g) were mixed at room temperature without the subsequent aging typically used in the conventional "Brode's method".[35] The mixture was stirred for 24 h. Washing, filtration, and cleaning were performed in the same way described by Brodie. Graphene oxide was collected through a precipitation method and evaluation of the solution. The resulted graphene oxide (GO) sheets were further reduced through hydrazine treatment.

GO (10 mg) was loaded in a 250 mL beaker, and deioned water (150 mL) was subsequently added, yielding an inhomogeneous yellow−brown dispersion. This dispersion was under ultrasonic processing by Misonix sonicator 3000 for 1.5 h at power 40 W. Hydrazine hydrate (20 mL, aqueous solution with concentration 35 wt %, Sigma-Aldrich) was then added, and the solution was stirred for a few minutes. Subsequently, the solution was transferred to a rotate evaporator (Rotovapor R210, Buchi, Germany) with an oil bath. The oil bath was heated to 95 °C, and the flask was rotated at a speed of 120 rpm under water reflux. The process was kept for 1 h. This produce was subsequently isolated by filtration over a medium-fritted glass funnel, washed copiously with water, and air-dried. The resulting solid was dispersed into distilled water under ultrasonic processing again and subjected to centrifugation for 30 min at 3000 rpm. The supernatant solution was used to produce a thin film by the filtration system. The resulting film was used for the measurement of the contact angle with a FTA1000 instrument (First Ten Angstroms, Portsmouth, VA). A total of 10 μL of liquids was placed on samples by a microsyringe, and the images of the liquid droplet were obtained instantaneously using a digital camera. The tangent lines to the droplets from the droplet and baseline were drawn in the images, and the angle between the tangent lines indicates the contact angle of the solid and liquid interface.

Powder X-ray diffraction [Rigaku Ultima III diffractometer, 40 kV, 44 mA, with Cu Kα (λ = 1.54 Å)] was used to fit the average interlayer distance in these GOs and reduced GO, and data were collected at room temperature over the range $2° \leq 2\theta \leq 55°$.

Solid GO powder was ground with a pestle and mortar and then dispersed into distilled water solution through an ultrasonic process under a power of 30 W for 30 min. The solution was sampled and dropped on the silicon substrate. The dried silicon substrate was examined by an atomic force microscope (Multimode SPM, Veeco, Inc.) at the tapping mode.

The Fourier transform infrared (FTIR) spectra of graphite, GO, and graphine samples were recorded using Spectrum-One equipped with an universal attenuated total reflectance (UATR) accessory (Perkin-Elmer, Waltham, MA). The UATR−FTIR was equipped with a ZnSe−diamond crystal composite that allows for the collection of FTIR spectra directly on a sample without any special preparation. The instrument is equipped with a "pressure arm", which is used to apply a constant pressure to the samples positioned on top of the ZnSe−diamond crystal to ensure a good contact between the sample and the incident IR beam and prevent the loss of the IR beam. The amount of pressure applied is monitored by the Perkin-Elmer FTIR software. FTIR spectra were collected at a spectrum resolution of 4 cm^{-1}, with 32 co-added scans over the range from 4000 to 650 cm^{-1}. A background scan of clean ZnSe−diamond crystal was acquired before scanning the samples.

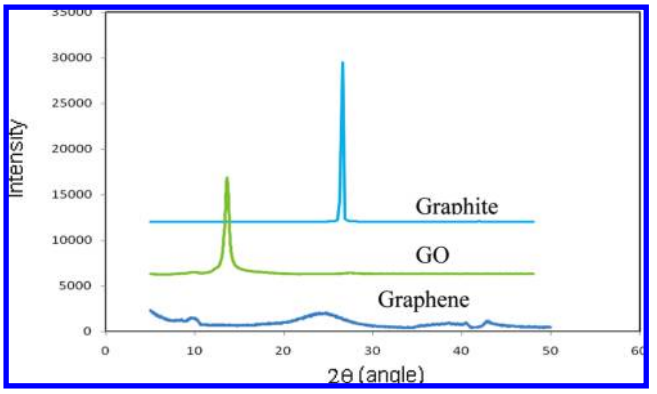

Figure 1. WXRD of graphene materials.

Results and Discussion

Wide-angle X-ray diffraction (WXRD) characterization results of pristine graphite GO and GNS are shown in Figure 1.

For the pristine graphite sample, the (002) peak appears at 27°, indicating an interlayer spacing of 0.34 nm. After oxidization-induced expansion, the (002) peak shifts to 12°, suggesting that the interlayer distance increased to 0.72 nm. These results are consistent with the data reported in the literature.[36−38] After hydrazine reduction and subsequent ultracentrifugation, the resulting graphene nanosheets from GO reduction did not show any sharp peak similar to GO and graphite but show a very weak and broad peak near 25°. This may stem from the change of the lattice structure. Reduced GO was exfoliated into a monolayer or few-layer states, and this kind of lattice structure is significantly different from the pristine graphite crystal.

The aqueous solution of exfoliated graphene sheets was dropped onto a silicon substrate and characterized by an atomic force microscope (AFM). The thickness of suspended graphene sheets was measured by section analysis, as shown in Figure 2. The measurement indicates that their thickness is 0.8−1.6 nm, suggesting that graphene in a monolayer or few-layer state was achieved. This result agrees with the literature report regarding exfoliated graphene.[36−39] Generally, single-layer graphene is always ~1 nm thick in AFM images because of the following reasons: attached molecules on the graphene surface, imperfect interface between the graphene and silicon substrate, and possible different attraction force between AFM probes as compared to the silicon substrate.[39]

Graphite, GO, and chemically reduced graphene were also characterized by FTIR in the mid-infrared range, and the results are shown in Figure 3. For the graphite spectrum, no vibration peak is observed. However, several vibration peaks were observed in the GO spectrum. The absorption peaks at 869.9, 928.1, and

(33) Ozcan, C.; Hasirci, N. *J. Appl. Polym. Sci.* **2008**, *108*, 438–446.
(34) Zhang, X. L.; Yang, D.; Xu, P.; Wang, C. C.; Du, Q. G. *J. Mater. Sci.* **2007**, *42*, 7069–7075.
(35) Jeong, H. K.; Lee, Y. P.; Lahaye, R. J. W. E.; Park, M.-H.; An, K. H.; Kim, I. J.; Yang, C.-W.; Park, C. Y.; Ruoff, R. S.; Lee, Y. H. *J. Am. Chem. Soc.* **2008**, *130*, 1362–1366.
(36) Xu, C.; Wu, X. D.; Zhu, J. W.; Wang, X. *Carbon* **2008**, *46*, 386–389.
(37) H.-Alonso, M.; Abdada, A. A.; McAllister, M. J.; Aksay, I. A.; Prud'homme, R. K. *Langmuir* **2007**, *23*, 10644–10649.
(38) Szabo, T.; Berkesi, O.; Forgo, P.; Josepovits, K.; Sanakis, Y.; Petridis, D.; Dekany, I. *Chem. Mater.* **2006**, *18*, 2740–2749.
(39) Li, X. L.; Wang, X. R.; Zhang, L.; Lee, S. W.; Dai, H. J *Science* **2008**, *319*, 1229–1232.

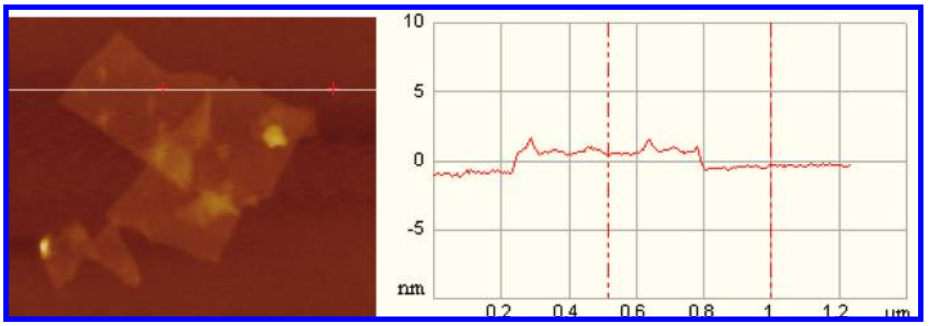

Figure 2. Tapping-mode AFM image of suspended graphene sheets.

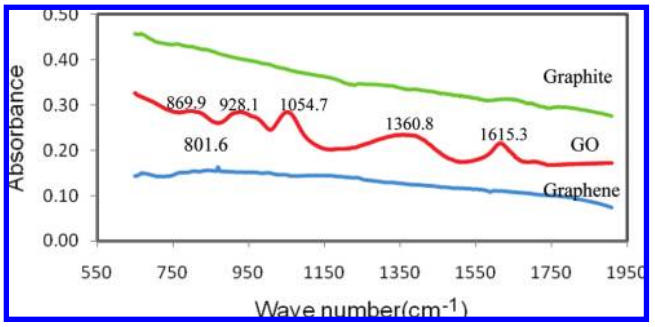

Figure 3. FTIR of graphene materials.

1054.7 cm^{-1} are attributed to the epoxy group.[40−42] The vibration peak at 1360 cm^{-1} is attributed to C−OH stretching.[36,38] The sharp peak at 1615 cm^{-1} is attributed to the adsorbed water molecules. The presence of these vibrations is indicative of the successful attachment of epoxide and hydroxyl. After hydrazine reduction, it is very interesting to note that all of these vibration peaks present at the GO spectrum disappeared. The FTIR results confirmed that isolated GO has been successfully converted to graphene sheets.

Graphite, GO, and graphene (chemically reduced GO) were assembled into a thin film by the filtration process, as described in the literature.[43−45] Each film was used to test the wettability by measuring its static contact angle with water. It was found that the static contact angle between graphite film and water is 98.3°. Because graphite consists of carbon atoms without any polarity, it demonstrates the hydrophobic properties. GO film was made from oxidized and isolated graphite. The measurement indicated that the static contact angle is 67.4°, much less than 90°. Hence, GO shows a good hydrophilic property. As indicated in FTIR results, the GO surface was grafted with hydroxyl and epoxy groups. These polar groups change the graphite properties from hydrophobic to hydrophilic. After chemical reduction of GO by hydrazine, hydroxyl and epoxy groups have been eliminated, as indicated by FTIR results. This is also in agreement with reported literature.[46,47] The experimental results indicated that the contact angle is 127.0°, which is larger than 90°. It is interesting to note that this contact angle is larger than that of graphite film and water. Even though isolated graphene also shows hydrophobic property, aqueous wettability is less than graphite.

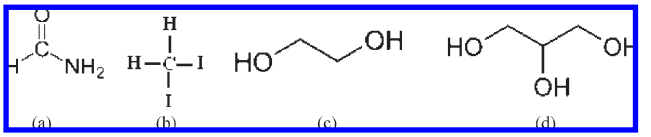

Figure 4. Molecular structures of polar solvents: (a) formamide, (b) diiodomethane, (c) ethylene glycol, and (d) glycerol.

In addition, the wettability of other polar organic solvents was also investigated. For the selected organic solvents, their molecular structures are listed in Figure 4.

These solvents demonstrate different polarity depending upon the polarity groups. Because of various polarities, graphene shows different wettability. The static contact angle measurement results are all based on a 2 s image. The static contact angles are listed in Table 1. For GO sheets, they are wettable to all of these polar solvents because the contact angles are all less than 90°. The graphene film is still not wettable to the glycerol, while it is wettable to the others. For all of the solvents, graphene is less wettable than graphite because all of the corresponding contact angles of graphene and solvents are larger than that of graphite and solvents. It seems that isolating graphite to few- or single-layer graphene makes it difficult to wet.

On the basis of Young's equation, the contact angle can be given as follows:[48,49]

$$\gamma_s = \gamma_{sl} + \gamma_l \cos\theta \quad (1)$$

where γ_s, γ_l, and γ_{sl} represent the solid surface free energy, liquid surface free energy, and solid−liquid interfacial energy, respectively. θ is the contact angle between the solid surface and liquid.

On the hand, the work of adhesion between a solid surface and liquid can be described by eq 2[33,48,49]

$$W_{sl} = \gamma_s + \gamma_l - \gamma_{sl} \quad (2)$$

Combining eqs 1 and 2 results in eq 3

$$W_{sl} = \gamma_l(1 + \cos\theta) \quad (3)$$

According the Table 1 and eq 3, the work of adhesion between graphene materials and selected liquid solvents can be calculated and provided in Table 2.

Because of the polarity of the covalently bonded epoxy and hydroxyl groups, the work of adhesion of the graphene

(40) Mao, Y.; Gleason, K. K. *Langmuir* **2004**, *20*, 2484–2488.
(41) Vandijkwolthuis, W. N. E.; Franssen, O.; Talsma, H.; Vansteenbergen, M. J.; Vandenbosch, J. J. K.; Hennink, W. E. *Macromolecules* **1995**, *28*, 6317–6322.
(42) Wang, S. R.; Liang, R.; Wang, B.; Zhang, C. *Carbon* **2007**, *45*, 3047–3049.
(43) Wang, S. R. Functionalization of carbon nanotubes: Characterization, modeling and composites applications. Ph.D. Dissertation, Florida State University, Tallahassee, FL, 2006.
(44) Wang, S. R.; Liang, R.; Wang, B.; Zhang, C. *Carbon* **2009**, *47*, 53–57.
(45) Qiu, J. J.; Zhang, C.; Wang, B.; Liang, R. *Nanotechnology* **2007**, *18*, 275708–275719.
(46) Stankovich, S. D; Dikin, A.; Piner, R. D.; Kohlhaas, K. A.; Kleinhammes, A.; Jia, Y.; Wu, Y; Nguyen, S. T.; Ruoff, R. S. *Carbon* **2007**, *45*, 1558–1565.
(47) Park, S.; Ruoff, R. S. *Nat. Nanotechnol.* **2009**, *4*, 217–224.
(48) Bouali, B.; Ganachaud, F.; Chapel, J.-P.; Pichot, C.; Lanteri, P. *J. Colloid Interface Sci.* **1998**, *208*, 81–89.
(49) Singh, J.; Whitten, J. *J. Macromol. Sci., Part A: Pure Appl. Chem.* **2008**, *45*, 885–892.

Table 1. Average Contact Angle Measured by the Droplet on the Film Surface[a]

materials	water	formamide	diiodomethane	ethylene glycol	glycerol
graphite	98.3 (5.1)	45.4 (3.4)	21.9 (2.1)	55.9 (3.0)	66.6 (3.9)
graphene oxide	67.4 (1.1)	18.5 (7.6)	38.5 (3.2)	21.6 (3.3)	49.7 (4.7)
graphene	127.0 (4.0)	80.4 (7.2)	42.6 (2.4)	76.3 (5.1)	111.3 (6.4)

[a] The numbers in parentheses show the standard deviation.

Table 2. Work of Adhesion between Solid−Liquid Interfaces

materials	water (mJ/m^2)	formamide (mJ/m^2)	diiodomethane (mJ/m^2)	ethylene glycol (mJ/m^2)	glycerol (mJ/m^2)
graphite	62.6	99.4	97.9	75.4	89.8
graphene oxide	104.2	114.1	90.4	90.8	107.9
graphene	29.0	69.1	88.4	59.3	41.4

oxide−solvent interface is much larger in comparison to graphite and isolated graphene layers. In addition, the isolated graphene layers showed smaller adhesion energy to the solvents than graphite. This is consistent with previous contact angles. Hence, reducing material dimension from 3D to 2D may reduce the wettability and decrease the interfacial adhesion with liquids.

There are several approximation methods to estimate the solid surface energy through contact angles, such as Zisman and Saito approximation, geometric and harmonic mean approximation, Berthelot's approximation, Fowkes approximation, acid-based approximation.[33,50,51] However, almost all of these approximations are significantly dependent upon the choice of the liquids and have some limitations. Neumann proposed an "equation of state" theory to determine the solid surface free energy by making some corrections to the above approximation, and the calculation results seem more reasonable.[51−53] Here, Neumann's method is used to determine the surface free energy of graphene. On the basis of the equation of state theory, the contact angle between the solid and liquid is given as follows:[51−53]

$$\cos\theta = -1 + 2\sqrt{\frac{\gamma_s}{\gamma_l}}e^{-\beta(\gamma_s - \gamma_l)^2} \quad (4)$$

where γ_s and γ_l represent solid and liquid surface free energy, respectively. β is the constant coefficient related to a specific solid surface.

Reorganization of eq 4 results in the following equation:

$$\ln\left[\gamma_l\left(\frac{1+\cos\theta}{2}\right)^2\right] = -2\beta(\gamma_s - \gamma_l)^2 + \ln(\gamma_s) \quad (5)$$

Plotting the left-hand side of eq 5 against γ_l results in a parabola curve, and fitting with the second-order polynomial equation will help to determine the parameters β and γ_s. Plots of graphite, GO, and graphene are given in Figure 5.

The surface free energy at room temperature was derived as follows: graphite, 54.8 mJ/m^2; GO, 62.1 mJ/m^2; graphene, 46.7 mJ/m^2. Graphite surface energy derived here agrees very well with the reported literature.[54] Because of the covalent attachment of epoxy and hydroxyl groups, GO showed higher surface energy. On the contrary, the isolated graphene showed a low surface energy and came down about 14.8% in comparison to graphite. These results further supported the above discussion of wettability of solid materials and the work of adhesion for the solid−liquid interface.

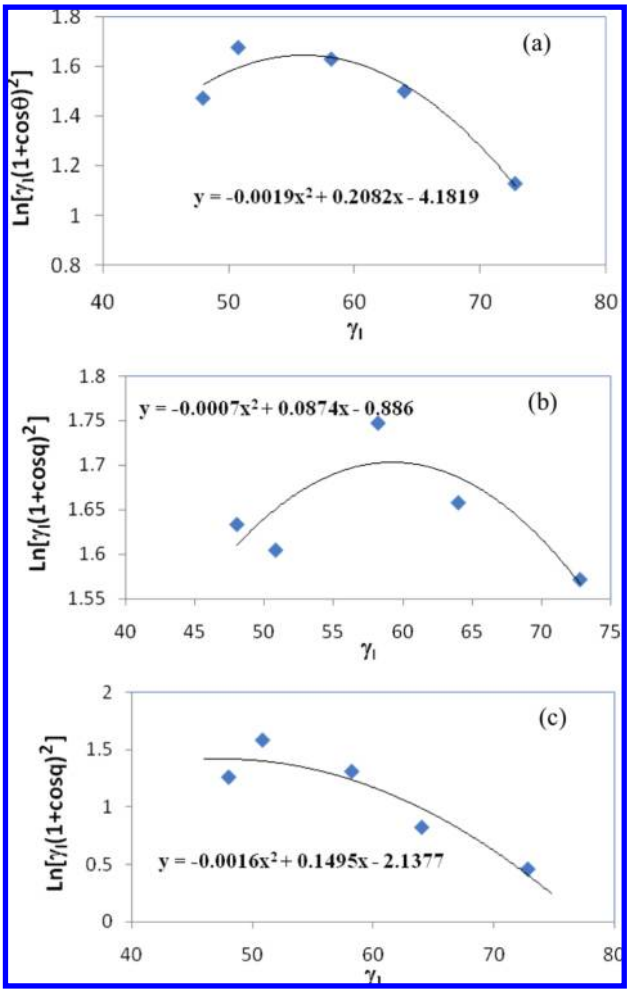

Figure 5. Plots of $\ln(\gamma_l(1+\cos\theta)/2)^2)$ versus γ_l for different liquids: (a) graphite materials, (b) GO materials, and (c) graphene materials.

Conclusions

Graphene sheets were produced through chemical exfoliation of natural graphite flake and hydrazine conversion. A range of liquids were used to test the wettability and measure the contact angles. It was found that a graphene oxide sheet is hydrophilic and a graphene sheet is hydrophobic. Preliminary results indicate that isolated graphene sheets are more difficult to wet than graphite and the work of adhesion between graphene and liquids is smaller in comparison to that of the graphite−liquid interface. Regression analysis of the measure results was carried out by the equation of state theory, and the surface free energy of graphene was determined. At room temperature, the graphene surface energy is 46.7 mJ/m^2, while oxidized graphene shows a surface energy of 62.1 mJ/m^2. These results will provide valuable guidance for the graphene-based biomedical devices, composites, and electronics.

Acknowledgment. The authors are grateful for the funding support from Texas Tech University.

Supporting Information Available: Original data of contact angle measurement. This material is available free of charge via the Internet at http://pubs.acs.org.

(50) Shimizu, R. N.; Demarquette, N. R. *J. Appl. Polym. Sci.* **2000**, *76*, 1831–1845.
(51) Chibowski, E.; Perea-Carpio, R. *Adv. Colloid Interface Sci.* **2002**, *98*, 245–264.
(52) Li, D.; Neumann, A. W. *Langmuir* **1993**, *9*, 50–54.
(53) Li, D.; Neumann, A. W. *J. Colloid Interface Sci.* **1992**, *148*, 190–200.
(54) Perez-Mendoza, M.; Almazan-Almazan, M. C.; Mendez-Linan, L.; Domingo-Garcia, M.; Lopez-Garzon, F. J. *J. Chromatogr., A* **2008**, *1214*, 121–127.